Etching polyimide with a nonequilibrium atmospheric-pressure plasma jet

J. Y. Jeong, S. E. Babayan, A. Schütze, and V. J. Tu
Chemical Engineering Department, University of California, Los Angeles, Los Angeles, California 90095

J. Park, I. Henins, and G. S. Selwyn
Plasma Physics, Los Alamos National Laboratory, Los Alamos, New Mexico 87545

R. F. Hicks[a)]
Chemical Engineering Department, University of California, Los Angeles, Los Angeles, California 90095

(Received 28 August 1998; accepted 26 March 1999)

An atmospheric-pressure plasma jet has been used to etch polyimide films at 1.0–8.0 ± 0.2 μm/min at 760 Torr and between 50 and 250 °C. The plasma was produced by flowing helium and oxygen between two concentric electrodes, with the inner one coupled to 13.56 MHz rf power and the outer one grounded. The etch rate increased with the O_2 partial pressure, the rf power and the substrate temperature. The apparent activation energy for etching was 0.16 eV. Langmuir-probe measurements revealed that the ion densities were between 1×10^{10} and 1×10^{11} cm^{-3}, 5 mm from the end of the powered electrode. Biasing the substrate had no effect on the rate. Ozone, singlet sigma metastable oxygen ($b\ ^1\Sigma_g^+$), and singlet delta metastable oxygen ($a\ ^1\Delta_g$) were detected in the plasma by emission spectroscopy. More ozone was produced in the effluent through the recombination of O atoms with O_2. Based on the production rate of O_3, the concentration of O atoms 6 mm from the powered electrode was estimated to be $\sim 7\times10^{14}$ cm^{-3} at 6.6 Torr O_2 and 200 W power. It is proposed that O atoms are the principal reactive species involved in etching polyimide. © *1999 American Vacuum Society.* [S0734-2101(99)01705-4]

I. INTRODUCTION

We have recently developed a new plasma source, the atmospheric-pressure plasma jet, which may have several applications in materials processing.[1–3] The jet is a nonequilibrium glow discharge: neutral temperatures range from 50 to 250 °C, while electron temperatures range from 1 to 4 eV.[3,4] Current-voltage measurements have revealed that the physics of this source is similar to a low-pressure gas discharge. With increasing current, the jet passes through a Townsend dark region, followed by normal glow and abnormal glow regions, and finally into an arcing mode. Normal and abnormal glow are observed at currents ranging from 0.01 to 1.00 A. The breakdown voltage of the atmospheric-pressure plasma jet is also quite low, between about 50 and 150 V, depending on the electrode design and the operating conditions. Reactive species are generated in the plasma that can be used to etch a variety of substrates, such as polyimide, silica, tantalum, and tungsten.[1] In addition, the source may be used for the plasma-enhanced chemical vapor deposition of silicon dioxide films at 150–350 °C and atmospheric pressure.[2,5]

Polyimide is used as a dielectric layer in microelectronic devices because it exhibits good thermal stability (glass transition ~300 °C), its dielectric constant is comparable to SiO_2 ($\epsilon = 3.4–4.1$), and it is generated in thin film form through reliable manufacturing processes.[6,7] For applications in the semiconductor industry, polyimide films must be patterned into precise submicron structures. For this reason, much research has focused on the plasma etching of this material.[8–15]

In order to assess the capabilities of the atmospheric-pressure plasma jet for materials processing, we have undertaken a detailed study of polyimide etching using oxygen and helium feed gases. Here, we report on the effect of the process conditions on the etch rate and on the composition of reactive species in the plasma. We have found that the jet produces ions, electrons, ozone, metastable molecular oxygen ($a\ ^1\Delta_g$ and $b\ ^1\Sigma_g^+$), and oxygen atoms. Our results suggest that the latter species is responsible for etching the organic film.

II. EXPERIMENTAL METHODS

Shown in Fig. 1 is a picture of the plasma jet during operation. A gas mixture of oxygen and helium was fed through an annular region between the two electrodes. The center electrode was biased with a rf generator operating at 13.56 MHz, while the outer electrode was grounded. The total gas flow rate was kept constant at 51 ℓ/min, while the rf power was varied from 150 to 550 W or the oxygen partial pressure was varied from 1.5 to 23.0 Torr. Raising the rf power from 150 to 550 W caused the gas temperature at the exit of the jet to increase from 50 to 225 °C. In order to control the sample temperature independently of the gas temperature, the polyimide films were mounted on a stage that was equipped with two 250 W cartridge heaters and a thermocouple, both of which were connected to a proportional integral differential (PID) controller. The plasma flowing past the electrodes exited through a nozzle, 6.4 mm in diameter, at a velocity of 26 m/s. The sample holder was placed 5–15 mm from the nozzle, and a circular aperture over the

a)Corresponding author; electronic mail: rhicks@ucla.edu

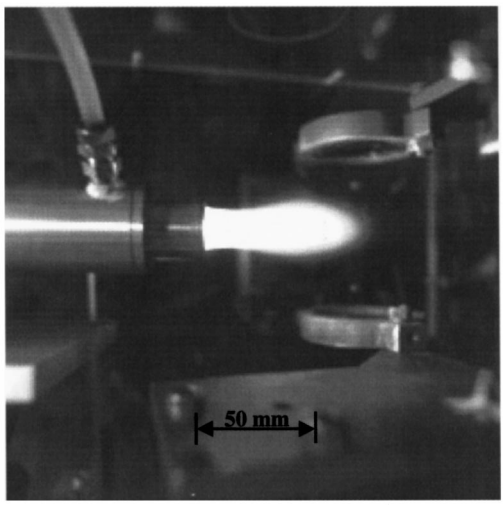

FIG. 1. Picture of the atmospheric-pressure plasma jet during operation. The bright plume is due to emission from electronically excited species.

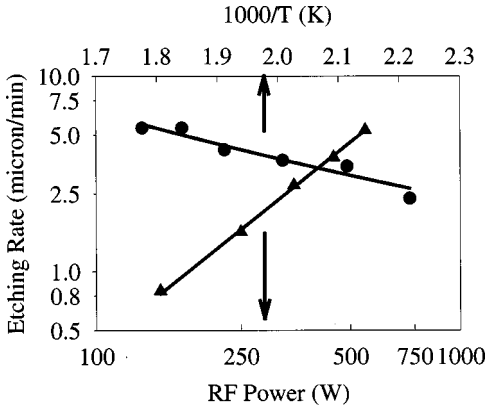

FIG. 2. Effect of rf power and substrate temperature on the kapton etch rate at 51.0 Å/min helium, 9.1 Torr O_2, and 5 mm jet-to-sample distance. For varying rf power the temperature, is equal to 275 °C, while for varying temperature, the rf power is equal to 200 W.

polyimide (kapton) film restricted the area etched to 71 mm^2. The etch rate was determined by measuring the film weight before and after each experiment.

Optical emission spectroscopy (OES) was used to detect electronically excited O atoms, O_2^+ ions, singlet sigma metastable $O_2(b\,^1\Sigma_g^+)$, and He atoms. The monochromator was equipped with a charge coupled device (CCD) camera having a resolution of 1 Å with a 150 μm entrance slit. A rectangular aperture placed above the jet effluent restricted the emission detected by the spectrometer to a cross section $1\times10\,mm^2$. A germanium infrared diode with a single-line filter was used to monitor the emission of singlet delta metastable oxygen $(a\,^1\Delta_g)$ at 1.27 μm. During these measurements, the rf power supply was pulsed by a square-wave generator at 1.6 Hz with a 50% duty cycle. The detector signal and pulse generator outputs were fed through a lock-in amplifier so that the background emission from the plasma could be eliminated. The ozone concentration was monitored by an electrochemical detector (GasTech, SC-90), using a stainless steel sampling tube of 1.6 mm inside/diam placed in the nozzle of the jet.

III. RESULTS

The effect of rf power on the kapton etch rate is shown in Fig. 2. The minimum rf power required for stable operation of the jet is 30 W. However, etch rates below 150 W are insignificant to within the experimental error (±0.2 μm/min). On the other hand, when the rf power exceeds 600 W, the plasma jet starts to arc. The data in Fig. 2 show that the reaction rate increases with the rf power. From the slope of the log-log plot, the dependence is $R_{etch}=P_{rf}^{1.5}$. Also, shown is the dependence of the etch rate on the substrate temperature. It obeys an Arrhenius relationship with an apparent activation energy of 0.16 ± 0.02 eV.

Presented in Fig. 3 is the effect of the oxygen partial pressure on the kapton etch rate. The reaction rate increases from 3 to 8 μm/min as the O_2 pressure is varied from 1.5 to 10.0 Torr. Upon raising the O_2 pressure from 10.0 to 23.0 Torr, no further change in the rate is recorded. The oxygen pressure could not be increased above 23.0 Torr because arcing will occur at the end of the electrodes.

Optical emission spectra taken inside the jet exhibit intense bands from electronically excited He and O atoms, metastable $O_2(b\,^1\Sigma_g^+)$, and O_2^+.[1] Examination of these spectra reveals He lines at 447.1, 501.6, 587.6, 667.8, 706.5, and 728.2 nm; O lines at 436.8, 533.1, 615.8, 645.6, 777.2, 794.8, 822.2, and 844.6 nm; a weak band of molecular oxygen ions at 580–640 nm; and a strong band for singlet sigma metastable O_2 at 758–770 nm $(b\,^1\Sigma_g^+O_2\rightarrow X\,^3\Sigma_g^-O_2)$.[16,17] By contrast, the emission spectra taken of the jet effluent contain a band for singlet sigma metastable O_2 and only a trace of the peaks for electronically excited He and O atoms.[1] No emission from ions is detected in the plasma jet effluent.

A planar Langmuir probe was used to measure the density of the charged particles in the plasma 5 mm downstream from the end of the powered electrode. When the probe is negatively biased by 100 V to the floating potential, a current of 3.5 μA is recorded. This current corresponds to an ion flux of 5×10^{13} particles/cm^2 s, which is about 100–1000 times lower than the fluxes measured in low-pressure capaci-

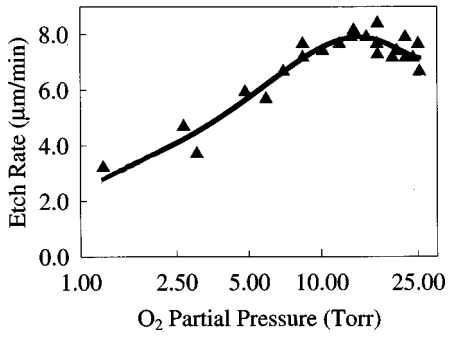

FIG. 3. Effect of oxygen partial pressure on the kapton etch rate at 51.0 Å/min helium, 500 W rf power, 250 °C film temperature, and 5 mm jet-to-sample distance.

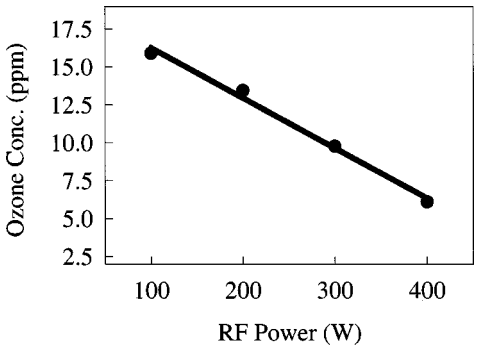

FIG. 4. Effect of rf power on the O_3 concentration at the nozzle for 51.0 ℓ/min helium and 3.0 Torr O_2.

tive discharges.[18] Evidently the etching process is not dominated or limited by ions.

The plasma jet also generates a considerable amount of ozone. The O_3 concentration at the exit of the nozzle increases rapidly with increasing O_2 partial pressure. A maximum ozone concentration of 225 ± 5 ppm is detected at 200 W rf power and 12.9 Torr O_2. Figure 4 shows the effect of the rf power on the O_3 concentration. A linear decrease occurs from 16 to 6 ppm as the power falls from 100 to 400 W. In Fig. 5, the influence of the gas temperature on the ozone concentration is illustrated. Here, the cooling water to the electrodes was turned off at $t=0$, and the gas temperature was allowed to rise under the action of the plasma. As the gas temperature increases from 143 to 168 °C, the ozone concentration drops from 165 to 75 ppm. Evidently the reactions involved in the production and/or consumption of ozone are highly activated.

Shown in Fig. 6 are the measured etch rate and the normalized emission intensities from the sigma and delta states of metastable oxygen as a function of the nozzle-to-sample distance. The reaction rate decreases rapidly from 4.3 ± 0.2 μm/min at 0 mm to 0.0 μm/min at 25 mm. Over the first 20 mm from the nozzle, the signal for sigma metastable O_2 decreases from its maximum value to less than the detection limit. By contrast, the signal for the delta metastable O_2 rises to a maximum at 20 mm and decays gradually over the next 100–200 mm. The difference in the decay rates of the metastable species is related to their lifetimes, which is

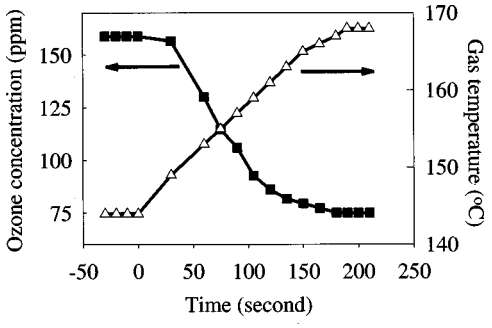

FIG. 5. Changes in O_3 concentration and gas temperature with time after the cooling water to the grounded electrode is shut off.

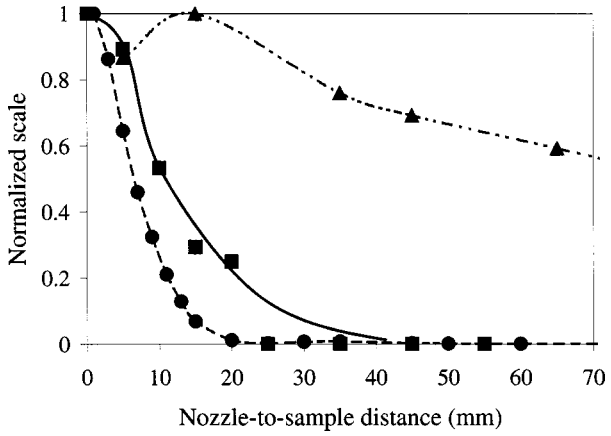

FIG. 6. Effect of jet-to-sample distance on the kapton etch rate [(■), max $=4.3$ μm/min] and the emission from the electronically excited delta (▲) and sigma (●) states of metastable oxygen.

~100 μs for $b\,^1\Sigma_g^+O_2$ and ~100 ms for $a\,^1\Delta_gO_2$.[19] Although not shown in Fig. 6, the ozone concentration was measured 0, 15, and 30 mm from the nozzle with an electrochemical ozone detector. The O_3 concentration increases with distance from 27.6 ppm (7.0×10^{14} cm^{-3}) at 0 mm to 56.2 ppm (1.4×10^{15} cm^{-3}) at 30 mm. Note that this trend is opposite to that of the etch rate, which rapidly declines with distance.

IV. DISCUSSION

Our experiments have shown that metastable molecular oxygen and ozone are produced in the plasma jet. We now consider whether these species are responsible for etching the kapton film. As can be seen in Fig. 6, the emission intensity for sigma metastable O_2 tracks the decline in etch rate with distance, whereas the delta metastable O_2 does not. Nevertheless, in separate experiments, it was found that the emission intensity from the sigma state decreases with the oxygen partial pressure, which is the reverse of the dependence of the etch rate on this variable (see Fig. 3). Moreover, previous studies of the reactivity of metastable oxygen with organic compounds have shown that sigma metastable oxygen is unreactive, and converts into the delta state upon collision with other molecules.[20] Thus, it may be concluded that neither sigma nor delta metastable oxygen is responsible for etching the polymer film.

Ozone could participate in polyimide etching, since it oxidizes a wide variety of organic compounds and, in combination with ultraviolet (UV) irradiation, is used to etch photoresist.[21] However, the ozone concentration in the plasma jet effluent is never high enough to result in a significant reaction rate. The highest concentration achieved in our study was 225 ppm. This quantity is 50–100 times less than that used in commercial UV/ozone etching processes.[21] In addition, the polyimide etch rate and the ozone concentration do not follow the same trends as the plasma process conditions. The rate goes up with rf power, while the O_3 concentration goes down with rf power. Also, the gas temperature strongly influences the O_3 concentrations, as shown in Fig. 5,

whereas the reaction rate is fairly insensitive to this variable. Therefore, we conclude that ozone is not responsible for etching kapton.

Alternatively, oxygen atoms could be the active etchant species. This species must be present in the jet effluent for ozone to be produced. The reaction of O with O_2 generates O_3 as follows:

$$O+O_2+M\rightarrow O_3+M,$$

$$k_1=1.4\times10^{-33}\ (\mathrm{cm^6/molecule^2\,s})\ \text{(Ref. 22)}. \tag{1}$$

Here, M is a third body, i.e., helium atoms. For the third body collision with O_2, the collision efficiency increases by a factor of 2.5. The O atoms are consumed by two other reactions as well:

$$O+O+M\rightarrow O_2+M,$$

$$k_2=2.5\times10^{-33}\ (\mathrm{cm^6/molecule^2\,s})\ \text{(Ref. 22)}. \tag{2}$$

$$O+O_3\rightarrow 2O_2,$$

$$k_3=8.5\times10^{-15}\ (\mathrm{cm^3/molecule\,s})\ \text{(Ref. 22)}. \tag{3}$$

Assuming the concentrations of oxygen atoms and ozone are between 1×10^{14} and $1\times10^{15}\,\mathrm{cm^{-3}}$ at 8 Torr O_2 pressure, then the rate of reaction (1) is two to three orders of magnitude higher than that of reactions (2) and (3). Consequently, without the generation of oxygen atoms in the plasma effluent, one may conclude that the increase in the ozone concentration with downstream distance corresponds to an equivalent decrease in the concentration of oxygen atoms.

To obtain an estimate of the O atom concentration in the jet effluent as a function of distance, the following mass balances for O_3, O, and O_2 were solved:

$$v_z\cdot\frac{d[O_3]}{dz}=k_1\cdot[O]\cdot[O_2]\cdot\beta\cdot[M]-k_3\cdot[O]\cdot[O_3], \tag{4}$$

$$v_z\cdot\frac{d[O]}{dz}=-k_1\cdot[O]\cdot[O_2]\cdot\beta\cdot[M]-2k_2\cdot[O]^2\cdot\beta\cdot[M]-k_3\cdot[O]\cdot[O_3], \tag{5}$$

$$v_z\cdot\frac{d[O_2]}{dz}=-k_1\cdot[O]\cdot[O_2]\cdot\beta\cdot[M]+k_2\cdot[O]^2\cdot\beta\cdot[M]+2k_3\cdot[O]\cdot[O_3]. \tag{6}$$

In these equations, v_z is the flow velocity (26 m/s); z is the distance downstream (mm); $[O]$, $[O_2]$, and $[O_3]$ are the concentrations of each of these species ($\mathrm{cm^{-3}}$); $[M]$ is the gas density ($\mathrm{cm^{-3}}$); and β is the ratio of the collision efficiency of helium to that of air at 100 °C (0.71).[23] Plug flow of the gas is assumed through the use of these equations, which is not unreasonable given that the Peclet number is around 570. Equations (4)–(6) have been solved using the Runge–Kutta method. The initial concentration of O_2 is that of the feed, since the conversion is less than 1% in the plasma. The initial concentration of O atoms is specified so as to give the best fit of the O_3 concentration to that measured experimentally.

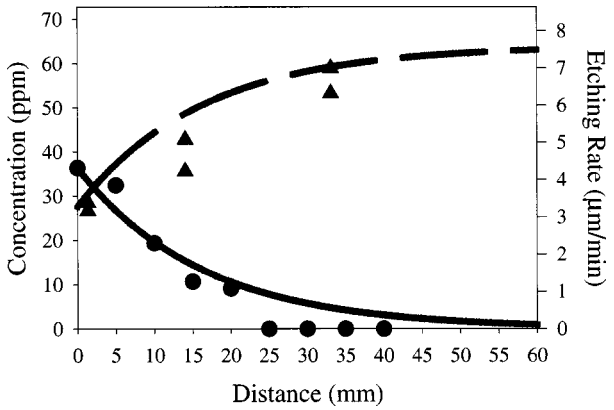

FIG. 7. Effect of jet-to-sample distance on the kapton etch rate (●), measured ozone concentration (▲), and calculated concentrations of O atoms (solid line) and ozone (dashed line).

Shown in Fig. 7 are the concentrations of oxygen atoms and ozone calculated from the numerical model. Also shown for comparison are the measured concentration of ozone and the etch rate of kapton. The theoretical results are given by solid curves, while the experimental data are given by symbols. Examination of Fig. 7 reveals that a good fit of the model to the actual concentration of ozone is achieved. In addition, the concentration of oxygen atoms follows the same trend with distance as the etch rate, suggesting that this species is indeed responsible for the etching reaction.

The calculated concentration of O atoms is on the order of $1\times10^{15}\,\mathrm{cm^{-3}}$, which is equal to about 0.5% of the oxygen fed. If every O atom colliding with the kapton film goes on to react with it, then this quantity of oxygen atoms is more than enough to account for the observed reaction rate. Although these results tend to support the conclusion that oxygen atoms are the primary etchant species, further work is needed to confirm this finding. In the future, we plan to measure O atom concentrations directly by injecting NO into the effluent gas and measuring the production of NO_2. In addition, a more sophisticated model will be developed, and simulations will be run over a wide variety of process conditions.

It is instructive to compare the polyimide etching results obtained with the plasma jet to those obtained in low-pressure gas discharges. It has been found that in the latter processes, the etch rate increases with the oxygen partial pressure, the rf power, and the substrate temperature. In the case of the oxygen partial pressure, a maximum rate is observed at about 0.2 Torr of O_2, after which the rate gradually declines with further increases in pressure.[24] These results are analogous to those obtained in the present study with the plasma jet. We observe a maximum in the etch rate at about 10 Torr of O_2, after which the rate slowly falls off. The apparent activation energy of etching with the plasma jet is 0.16 eV, in good agreement with earlier studies using low-pressure plasmas. In those studies, values ranging from 0.05 to 0.26 eV have been reported.[25,26] The close correlation between the operation of the atmospheric-pressure plasma jet and low-pressure gas discharges suggests that the mechanism

of polyimide etching is the same in both cases.

A number of researchers have shown that oxygen atoms are responsible for etching organic polymer films in low-pressure plasmas.[18,27–29] Cook and Benson[30] employed electron paramagnetic resonance spectroscopy to directly measure the oxygen atoms and excited oxygen molecules downstream from the cavity in a microwave asher. They concluded that oxygen atoms are the key reactive species, rather than excited oxygen molecules, since the activation energy for etching is identical to the activation energy for the loss of oxygen atoms. In addition, they confirmed that the loss of oxygen atoms is not due to a variation in the recombination rate with temperature by observing no change in the loss rate when a ceramic sample was substituted for the photoresist. Spencer *et al.*[31] compared the rates of photoresist etching in a pure O_2 plasma and in a N_2O/O_2 plasma. Nitrous oxide provides an additional source of oxygen atoms, but not excited oxygen molecules. Although the etch rate was higher with the mixture than with pure O_2, the activation energy stayed constant, suggesting that the increase in rate is not due to different surface reactions, but solely to an increase in the concentration of oxygen atoms. Given that the plasma jet behaves in a fashion analogous to that of low-pressure plasmas, we may surmise that oxygen atoms are most likely the reactive species involved in the atmospheric-pressure plasma etching of polyimide.

V. CONCLUSIONS

An atmospheric-pressure plasma jet has been developed for use in materials processing. Using oxygen and helium feed gases, this source is able to etch polyimide films at rates up to 8 μm/min at 250 °C. The close similarity between this process and the low-pressure plasma etching of polymers suggests that the reaction mechanism is the same in both cases, i.e., that O atoms impinge upon the surface of the organic film and convert it into carbon oxides and water.

ACKNOWLEDGMENTS

This work was conducted under the auspices of the U.S. Department of Energy, supported in part by funds provided by the University of California, and in part by funds provided by Basic Energy Sciences, Environmental Management Sciences Program, and by the Office of Science and Risk Policy (Award No. DE-F5607-96ER45621). Two of the authors (J.Y.J. and S.E.B.) are grateful for fellowships from the University of California Center for Environmental Risk Reduction and the Toxic Substances Research and Training Program. Also, another author (A.S.) is grateful for a fellowship from the Deutsche Forschungsgemeinschaft (DFG).

[1] J. Y. Jeong, S. E. Babayan, V. J. Tu, J. Park, I. Henins, J. Velarde, R. F. Hicks, and G. S. Selwyn, Plasma Sources Sci. Technol. **7**, 282 (1998).
[2] S. E. Babayan, J. Y. Jeong, V. J. Tu, J. Park, R. F. Hicks, and G. S. Selwyn, Plasma Sources Sci. Technol. **7**, 286 (1998).
[3] A. Schütze, J. Y. Jeong, S. E. Babayan, J. Park, G. S. Selwyn, and R. F. Hicks, IEEE Trans. Plasma Sci. **26**, 1685 (1998).
[4] J. Y. Park (unpublished results).
[5] S. E. Babayan, J. Y. Jeong, A. Schütze, V. J. Tu, G. S. Selwyn, and R. F. Hicks, J. Vac. Sci. Technol. A. (submitted).
[6] A. M. Wilson, *Polyimides: Synthesis, Characterization, and Applications*, edited by K. L. Mittel (Plenum, New York, 1982), Vol. 2, p. 715.
[7] G. Samuelson and S. Lytle, in Ref. 6, p. 751.
[8] A. M. Wilson, Thin Solid Films **83**, 145 (1981).
[9] G. Samuelson, *Polymer Materials for Electronic Applications*, ACS Symp. Ser. No. 184 (American Chemical Society, Washington, DC, 1982), p. 93.
[10] Y. K. Lee and J. D. Craig, in Ref. 9, p. 107.
[11] J. C. Bolger, in Ref. 9, p. 871.
[12] D. R. Day, D. Ridley, J. Mario and S. D. Senturia, in Ref. 6, p. 767.
[13] C. C. Chao and W. V. Wang, in Ref. 6, p. 783.
[14] T. O. Herndon, R. L. Burke and W. J. Landoch, in Ref. 6, p. 809.
[15] J. Tkach, in Ref. 6, p. 841.
[16] G. Herzberg, Nature (London) **133**, 759 (1934).
[17] L. M. Branscomb, Phys. Rev. **86**, 258 (1952).
[18] D. L. Flamm and G. K. Herb, in *Plasma Eching, An Introduction*, edited by D. M. Manos and D. L. Flamm (Academic, San Diego, CA, 1989).
[19] E. A. Ogryzlo, *Singlet Oxygen: Reactions with Organic Compounds and Polymers*, edited by B. Ranby and J. F. Rabek (Wiley, London, 1978).
[20] R. P. Wayne, *Singlet O_2*, edited by A. A. Frimer (Chemical Rubber, Boca Raton, FL, 1985), Vol. I, p. 81.
[21] P. C. Wood, T. Wydeven, and O. Tsuji, *Surface Chemical Cleaning and Passivation of Semiconductor Processing Symposium*, edited by G. S. Higashi, E. A. Irene, and T. Ohmi (Materials Research Society, Pittsburgh, PA, 1993), p. 237.
[22] *Reaction Rate and Photochemical Data for Atmospheric Chemistry–1977*, edited by R. F. Hampson, Jr. and D. Garvin (National Bureau of Standards, Washington DC, 1978).
[23] W. C. Gardiner and J. Troe, *Combustion Chemistry*, edited by W. C. Gardiner, Jr. (Springer, New York, 1984).
[24] B. Lamontagne, A. M. Wrobel, G. Jalbert, and M. R. Wertheimer, J. Phys. D **20**, 844 (1987).
[25] V. Vukanovic, G. A. Takacs, E. A. Matuszak, F. D. Egitto, F. Emmi, and R. S. Horwath, J. Vac. Sci. Technol. B **6**, 66 (1988).
[26] J. Paraszczak, M. Hatzakis, E. Babich, J. Shaw, E. Arthur, E. Grenon, and M. de Paul, Microelectron. Eng. **2**, 517 (1984).
[27] M. A. Lieberman and A. J. Lichtenberg, *Principles of Plasma Discharges and Materials Processing* (Wiley, New York, 1994).
[28] O. Joubert, J. Pelletier, and Y. Arnal, J. Appl. Phys. **65**, 5096 (1989).
[29] J. F. Battey, IEEE Trans. Electron Devices **ED-24**, 140 (1977).
[30] J. M. Cook and B. W. Benson, J. Electrochem. Soc. **130**, 2459 (1983).
[31] J. E. Spencer, R. L. Jackson, and A. Hoff, in *Proceedings of the Symposium on Plasma Processes*, edited by G. S. Mathad, G. C. Schwartz, and R. A. Gottscho (The Electrochemical Society, Pennington, NJ, 1987), p. 186.